

ELECTRICAL CONDUCTION AND BREAKDOWN IN SOL-GEL DERIVED PZT THIN FILMS

Reza Moazzami, Chenming Hu, and William H. Shepherd[†]
Department of Electrical Engineering and Computer Sciences
University of California, Berkeley, CA 94720
[†]National Semiconductor, Santa Clara, CA 95052

Abstract

PZT films with equal titanium and zirconium concentrations were prepared by sol-gel deposition. For DRAM operation, the equivalent SiO_2 thickness of a 4000Å PZT film is less than 17Å. The low-field resistivity and its activation energy are $3.5 \times 10^{10} \Omega\text{-cm}$ and 0.33 eV, respectively. For the same capacitor polarization, the electrical conduction and time-dependent dielectric breakdown (TDDB) properties of PZT are superior to other proposed DRAM dielectrics. But for typical operating conditions, the TDDB characteristics require further improvement to ensure DRAM reliability.

Introduction

As dynamic random access memory (DRAM) density continues to increase, the required storage capacitance per unit area poses a serious challenge to trench and stacked-capacitor cell technologies based on $\text{SiO}_2/\text{Si}_3\text{N}_4$. In order to meet the charge storage requirements, high dielectric constant materials such as tantalum pentoxide [1], [2] and yttrium oxide [3] have been proposed as alternatives to silicon dioxide and oxide/nitride/oxide (ONO) stacked structures. While the relative permittivity of these materials is three to six times that of SiO_2 , the net gain in charge storage density is only a factor of two or three at best because of the higher leakage current. In this paper, ferroelectric lead zirconate titanate ($\text{PbZr}_x\text{Ti}_{1-x}\text{O}_3$, commonly called PZT) is studied as a potentially attractive candidate for the storage dielectric in future DRAM technologies. The polarization, electrical conduction, and time-dependent dielectric breakdown behavior of PZT are presented and compared with other proposed dielectric structures.

Capacitance-Voltage Characteristics

4000Å PZT films ($x=0.5$) were prepared by sol-gel deposition and subsequent annealing above the crystallization temperature [4]. Platinum was used for both top and bottom electrodes. The resultant films exhibited ferroelectric behavior with a coercive field of 25 kV/cm and a remanent polarization of $150 \text{ fC}/\mu\text{m}^2$ ($15 \mu\text{C}/\text{cm}^2$) as shown in Figure 1.

Nonvolatile ferroelectric memory cells experience fatigue, a gradual loss of detectable polarization during continuous cycling [5], and are vulnerable to retention failure caused by dielectric aging [6], [7]. However, for DRAM operation, the ferroelectric only needs to be biased in one polarity thus possibly avoiding significant fatigue and long term retention is no longer required. In this case, the avail-

able polarization determined from a unipolar quasi-static C-V measurement is $140 \text{ fC}/\mu\text{m}^2$ for 5V operation (Figure 2) which is equivalent to a 7.5 Å SiO_2 film subjected to a 3V voltage swing. A DRAM cell typically requires 100 fC of stored charge to prevent soft errors.

It is evident that domain switching is occurring even in the unipolar case since there is significant hysteresis in the capacitance and polarization characteristics. In addition, the calculated polarization for a high to low ramp is slightly smaller than that for a low to high ramp. This

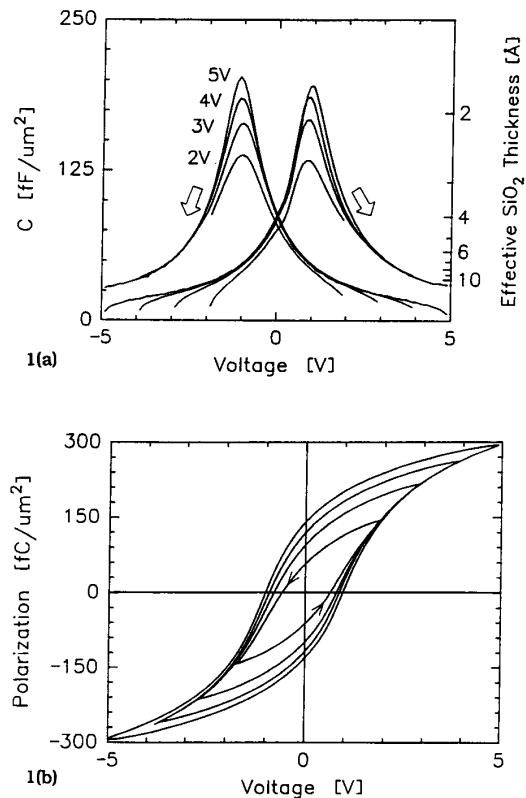


Figure 1. Ferroelectric switching of a 4000 Å PZT film obtained from a quasi-static voltage ramp. The peak-to-peak voltage varies from 2V to 5V. The polarization is comparable to only a few monolayers of SiO_2 .

difference is attributed to domain switching occurring during the ~1 second time period between the end of the high to low ramp and the beginning of the low to high ramp and should be considered unavailable for high speed DRAM operation. For voltages below 2V (twice the coercive voltage), the available polarization increases almost linearly with voltage. The polarization saturates fairly rapidly above 2V. For a 3V power supply, the effective SiO₂ film is approximately 10 Å. This estimate does not take into account the degradation in the available polarization which has been observed during both dc and pulse dc stressing [8].

A lower limit for the total polarization available for DRAM operation can still be obtained from the small-signal capacitance which exhibits virtually no degradation. Even in this worst case, the DRAM capacitor polarization at 3V is equivalent to a 17 Å SiO₂ film subjected to a 3V voltage swing (Figure 3b). Physically, the small-signal capacitance is attributed to nonferroelectric polarizability. However, the small hysteresis loop in Figure 3a shows that the ferroelectric domain structure has some influence on nonferroelectric polarizability.

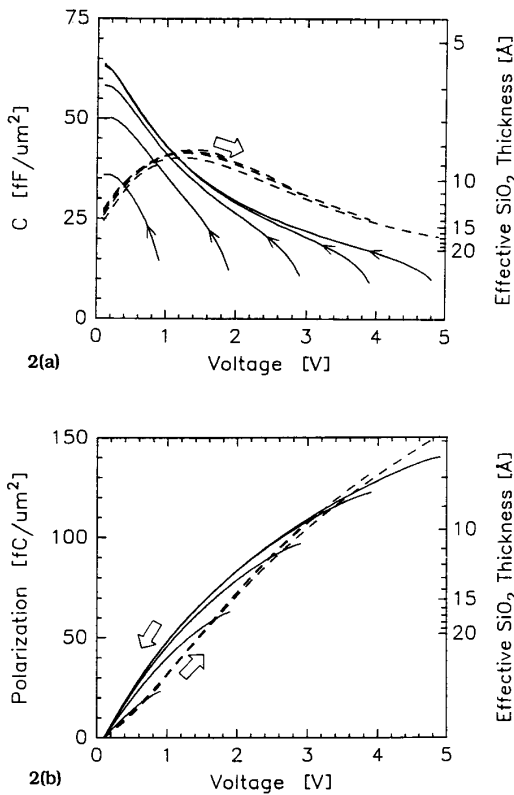


Figure 2. In order to minimize fatigue, ferroelectric switching is not performed during DRAM operation. For a 3V supply, the effective SiO₂ thickness is 10 Å (2b). The C-V curves shown are for peak voltages between 1V and 5V. The effective thicknesses plotted on the right side on Figures 2b and 3b are calculated assuming a 3V voltage swing.

Electrical Conduction

The leakage current characteristics exhibit ohmic behavior at low fields and exponential behavior at moderately high fields as shown in Figure 4. An expression of the form,

$$J \propto \sinh BE, \quad (1)$$

where J is the current density, E is the applied electric field, and B is a constant, provides a good fit to the data. A field dependence of this type has been derived for ionic conductivity assuming single-ion transport, symmetric ion-vacancy potentials, and a field-independent vacancy concentration [9]. In this case, J is expressed as

$$J = A \exp(-E_a/kT) \sinh(BE/kT) \quad (2)$$

where A is a constant (equal to 10 A/cm² for the data in Figure 4) and E_a (equal to 0.35 eV) is the activation energy. The coefficient, B , is proportional to the ionic charge, Ze , and the hopping distance, λ : $B = Ze\lambda/2$. Assuming a doubly-ionized species ($Z=2$) and $B = 0.057$ eV-cm/MV (from Figure 4b), the hopping distance is determined to be approximately 5.5 Å. The model considered here is hypothetical since no direct evidence exists for ionic conduction.

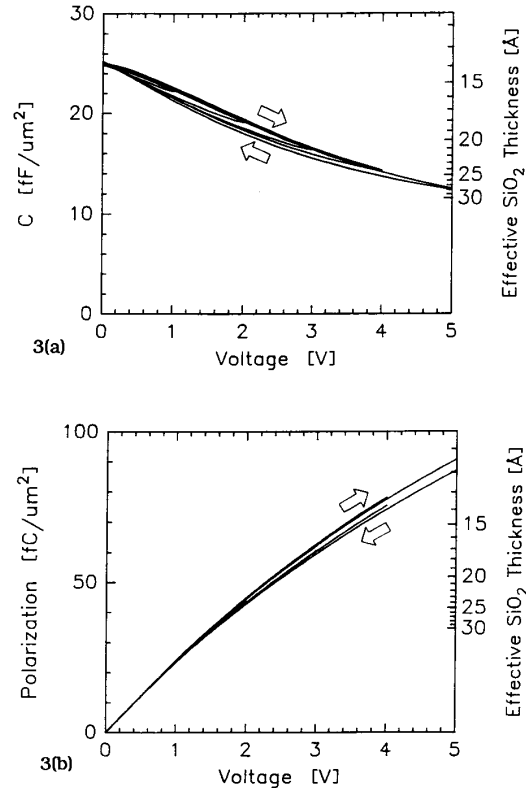


Figure 3. Even if aging causes polarization degradation, there is sufficient small-signal capacitance available. In this worst case, the effective SiO₂ thickness is 17 Å for a 3V supply. The C-V curves shown are for peak voltages between 1V and 5V.

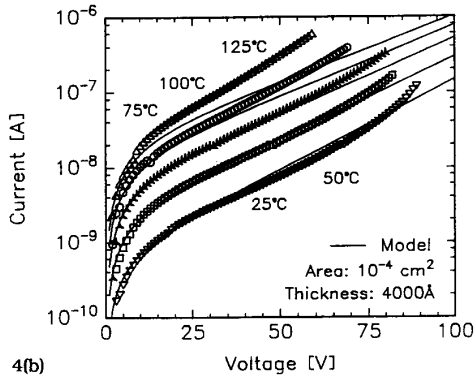
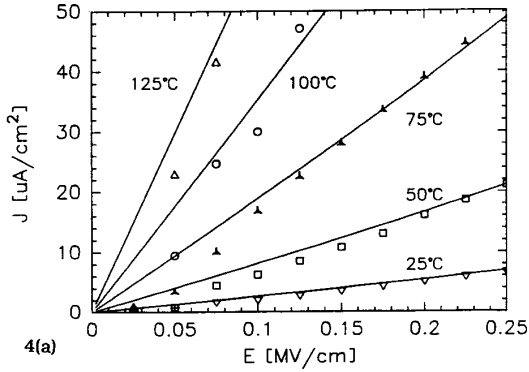


Figure 4. Electrical conduction in PZT films follows an ohmic relationship at low fields (4a) and an exponential field dependence at high fields (4b). The solid lines are based on a model for ionic conduction (Equation 2).

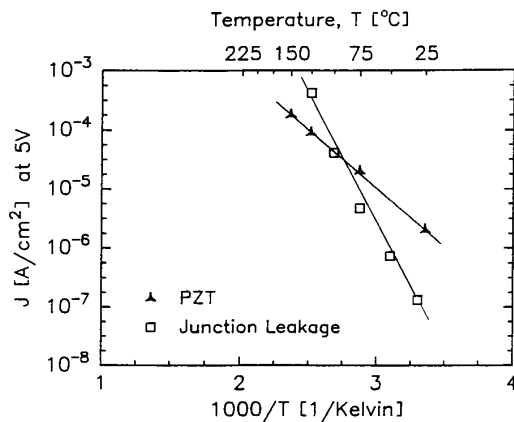


Figure 5. Since the activation energy for electrical conduction in PZT is less than 0.4eV, pn junction leakage dominates at high temperatures.

In the low-field limit, (2) reduces to the conventional ionic conduction relation [10]:

$$J = A \frac{BE}{kT} \exp\left[\frac{-E_a}{kT}\right]. \quad (3)$$

The low-field resistivity and activation energy determined from Figure 4a are $3.5 \times 10^{10} \Omega\text{-cm}$ and 0.33 eV in agreement with the A , B , and E_a determined using (2) and Figure 4b. Because of this low activation energy, the leakage current does not impose a serious limitation since at high temperatures pn junction leakage dominates (Figure 5).

Significant space charge effects are observable even at low fields. For example, after the application of a short stress, 10 seconds at 5V, on an unstressed capacitor, a dramatic drop in conductivity is detected (Figure 6). Repeated ramping from 0 to 30V causes progressively larger shifts in the I-V characteristics. This space charge accumulation does not appear to be due to the movement of a fixed amount of ionic charge since no hysteresis is observed in the I-V characteristics following polarity reversal: The I-V characteristics shift monotonically regardless of the polarity. However, following high temperature annealing, the conductivity does approach its initial unstressed value (Figure 7).

Figure 8 is a plot of the current density versus the silicon dioxide field, E_{eff} , needed to obtain the same capacitor polarization, $P = 3.9\epsilon_0 E_{eff}$. P/J is the capacitor discharge time constant. Because of its extremely large polarization, the PZT film exhibits superior leakage characteristics compared to other proposed dielectric structures [1]-[3], [11]. Similar to bulk PZT ceramics, adding the proper impurities suppresses the conductivity arising from oxygen and lead vacancies and can further increase the resistivity of PZT films [12]. For example, the resistivity of a lanthanum-iron modified $\text{PbZr}_{0.5}\text{Ti}_{0.5}\text{O}_3$ film is more than an order of magnitude greater than that of an unmodified film [8].

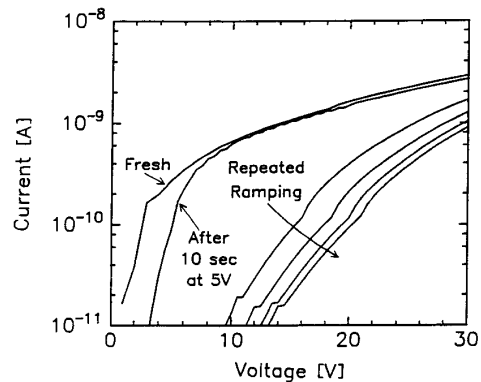
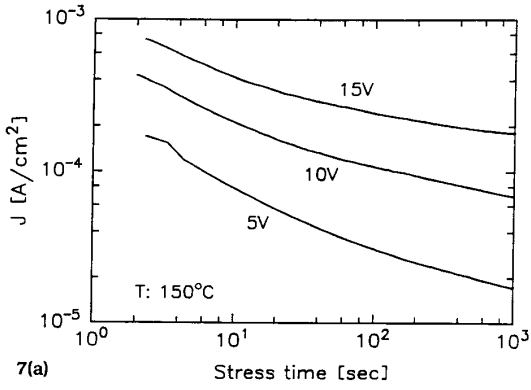
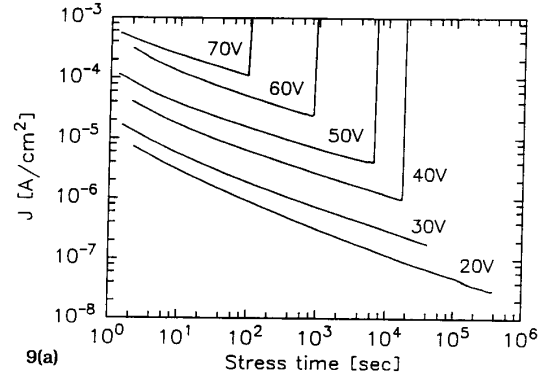


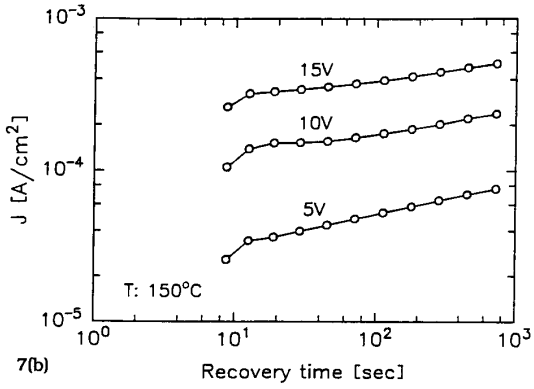
Figure 6. The conductivity of PZT films drops following successive voltage ramps.



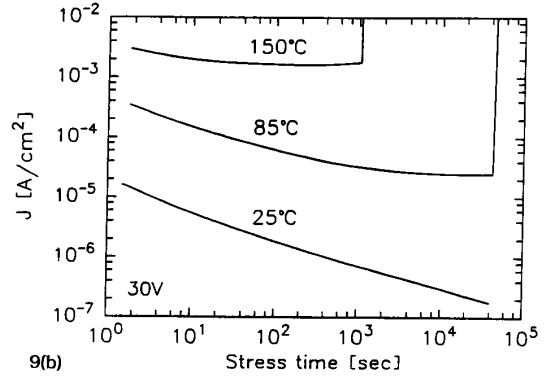
7(a)



9(a)



7(b)



9(b)

Figure 7. Constant voltage stressing also causes a drop in conductivity (7a). However, the conductivity approaches its original value after annealing at high temperature (7b).

Figure 9. The current density during room-temperature constant voltage stress is a power-law function of the stress time (9a). At higher temperatures, saturation and turn-around are observed (9b).

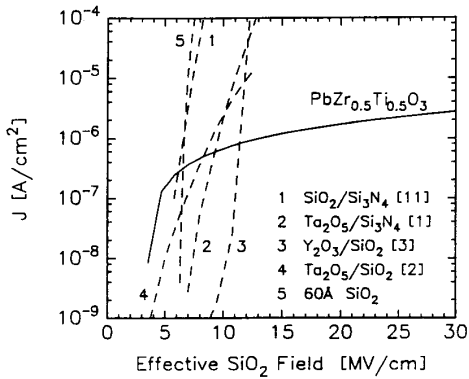


Figure 8. For the same capacitor polarization, the conduction characteristics of PZT are superior to other proposed DRAM dielectrics. For this comparison, an effective worst-case linear dielectric constant of 900 was used for PZT (determined from Figure 3b).

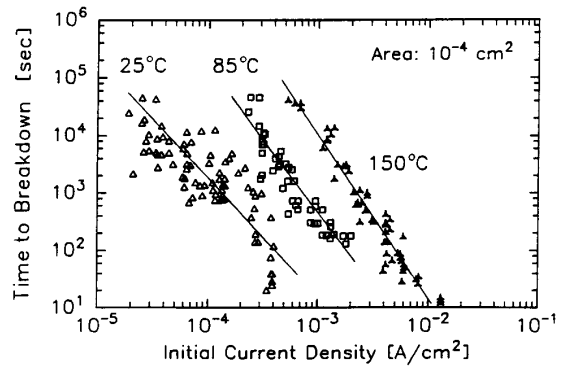


Figure 10. The time to breakdown for constant voltage stress is roughly proportional to $J^{-2.8}$ at 150°C and $J^{-2.0}$ at room temperature. The activation energy is approximately 0.6 eV.

Time-Dependent Dielectric Breakdown

The time-dependent dielectric breakdown behavior was studied to determine the viability of PZT films for DRAM applications. At room temperature, the current density during constant voltage stress decreases by several orders of magnitude before destructive breakdown (Figure 9a). This behavior appears to follow a power-law relationship. However, at higher temperatures, a turn-around is observed before breakdown (Figure 9b). The time to breakdown, t_{BD} , is plotted as a function of the current density in Figure 10; approximate power-law relationships are obtained. The lifetime is proportional to $J^{-2.8}$ at 150°C and $J^{-2.0}$ at room temperature. The average activation energy between room temperature and 150°C is approximately 0.6 eV and increases at low fields.

Lifetime projections are obtained by plotting the time to breakdown as a function of the stress voltage (Figure 11). Lifetime extrapolation based on an exponential field dependence yields lifetimes less than a month at 3V and 150°C. The electric field acceleration factor (defined as the slope of $\log t_{BD}$ versus the applied field) is approximately 4 decades per MV/cm. The extrapolated lifetime may be as high as 100 years at 150°C and 3V using an inverse-field law. Defect-related lifetimes may be much shorter and must be studied in the future. The actual field dependence and physical mechanism responsible for breakdown can not be determined easily from this data alone since space charge buildup during stressing causes very nonuniform internal fields. At the same effective electric field, the TDDB characteristics of PZT films are superior to other dielectrics as shown in Figure 12. However, assuming these films are used at typical supply voltages, TDDB appears to be the single most limiting factor for the use of PZT films in DRAMs.

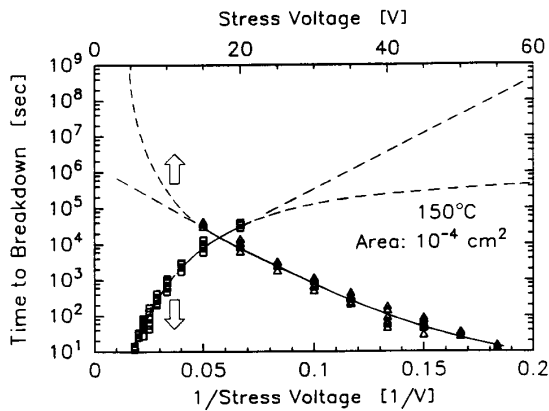


Figure 11. Time-dependent dielectric breakdown characteristics of PZT as a function of stress voltage. Extrapolation based on an inverse-field law (upper dashed curves) projects lifetimes much greater than 10 years under worst case operating conditions (3V, 150°C). However, projections based on an exponential field dependence (lower dashed curves) show that TDDB may be a very serious limitation for DRAM applications.

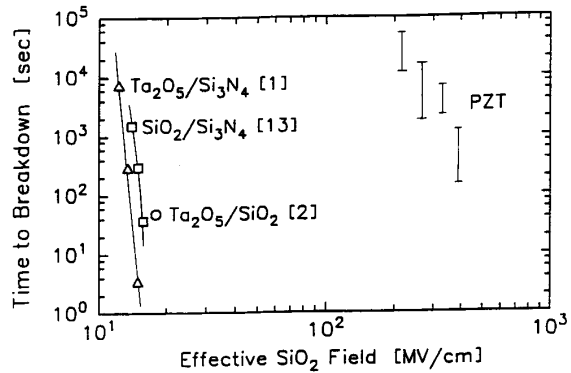


Figure 12. For the same capacitor polarization, the TDDB characteristics of PZT are superior to other proposed DRAM dielectrics.

Summary and Conclusions

The viability of PZT films for DRAM applications was discussed. 4000Å PZT films with an effective SiO₂ thickness less than 17Å were prepared by sol-gel deposition. The films exhibited ohmic behavior at low fields and exponential field dependence at high fields. The conduction characteristics can be modeled accurately using expressions derived for ionic conductivity. At the same effective SiO₂ field, the leakage and TDDB characteristics are superior to other dielectric structures. However, lifetime extrapolations to worst-case operating conditions show that TDDB may be a very serious limitation for DRAM applications. Optimization of material properties of PZT films, especially the TDDB lifetime, is necessary for reliable DRAM operation.

Acknowledgements

This research was sponsored by the Joint Services Electronics Program under contract F49620-87-0041. Reza Moazzami is supported by an IBM Doctoral Fellowship.

References

- [1] H. Shinriki, Y. Nishioka, Y. Ohji, and K. Mukai, "Oxidized Ta_2O_5/Si_3N_4 dielectric films for ultimate-STC DRAMs," *IEDM Tech. Dig.*, p. 684, 1986.
- [2] H. Shinriki, M. Nakata, Y. Nishioka, and K. Mukai, "Leakage current reduction and reliability improvement of effective 3nm-thick CVD Ta_2O_5 film by two-step annealing," *Tech. Dig. Symp. VLSI Tech.*, p. 25, 1989.
- [3] L. Manchanda and M. Gurvitch, "Yttrium oxide/silicon dioxide: a new dielectric structure for VLSI/ULSI circuits," *IEEE Electron Dev. Lett.*, vol. 9, no. 4, p. 180, April 1988.
- [4] S.K. Dey, K.S. Budd, and D.A. Payne, "Thin-film ferroelectrics of PZT by sol-gel processing," *IEEE Trans. Ultrasonics Ferroelectrics Freq. Control*, vol. 35, no. 1, p. 80, January 1988.
- [5] J. Carrano, C. Sudhama, J. Lee, A. Tasch, and W. Miller, "Electrical and reliability characteristics of lead-zirconate-titanate (PZT) ferroelectric thin films for DRAM applications," *IEDM Tech. Dig.*, p. 255, 1989.
- [6] J.T. Evans and R. Womack, "An experimental 512-bit nonvolatile memory with ferroelectric storage cell," *IEEE J. Solid-State Circuits*, vol. 23, no. 5, p. 1171, October 1988.
- [7] J.F. Scott, C.A. Araujo, H.B. Meadows, L.D. McMillan, A. Shawabkeh, "Radiation effects on ferroelectric thin-film memories: retention failure mechanisms," *J. Appl. Phys.*, vol. 66, no. 3, p. 1444, 1 August 1989.
- [8] R. Moazzami, C. Hu, and W.H. Shepherd, *to be published*.
- [9] J.J. O'Dwyer, *The Theory of Electrical Conduction and Breakdown in Solid Dielectrics*, Oxford: Clarendon Press, 1973, ch. 2, p. 18.
- [10] S.M. Sze, *Physics of Semiconductor Devices*, 2nd ed., New York: J. Wiley, 1981, ch. 7, p. 403.
- [11] Y. Ohno, A. Ohsaki, I. Ogoh, K. Kobayashi, M. Hirayama, and T. Kato, "Reliability of SiO_2/Si_3N_4 dielectric films on $MoSi_2$ and WSi_2 ," *Tech. Dig. Symp. VLSI Tech.*, p. 23, 1989.
- [12] B. Jaffe, W.R. Cook, and H. Jaffe, *Piezoelectric Ceramics*, New York: Academic Press, 1971, ch. 10, pp. 237-242.
- [13] Y. Ohji, T. Kusaka, I. Yoshida, A. Hiraiwa, K. Yagi, and K. Mukai, "Reliability of nano-meter thick multi-layer dielectric films on poly-crystalline silicon," *Proc. Int. Rel. Phys. Symp.*, p. 55, 1987.